Usability and Challenges of Offshore Wind Energy in Vietnam Revealed by the Regional Climate Model Simulation

Van Q. Doan[1], Van Nguyen Dinh[2], Hiroyuki Kusaka[3], Thanh Cong[4], Ansar Khan[5], Du Van Toan[6], and Nguyen Dinh Duc[7]

[1]*Center for Computational Sciences, University of Tsukuba, Tsukuba, Japan*
[2]*MaREI Centre for Marine and Renewable Energy, University College Cork, Cork, Ireland*
[3]*Center for Computational Sciences, University of Tsukuba, Tsukuba, Japan*
[4]*VNU Hanoi, University of Sciences, Hanoi, Vietnam*
[5]*Department of Geography, Lalbaba College, University of Calcutta, Kolkata, India*
[6]*Vietnam Institute of Seas and Islands, MONRE, Hanoi, Vietnam*
[7]*VNU Hanoi, University of Engineering and Technology, Hanoi, Vietnam*

Abstract

This study revealed great potential and shortcoming of offshore wind energy in Vietnam by numerical simulations with Weather Research and Forecasting (WRF) model at 10-km resolution for 10 years (2006−2015). The greatest energy potential was found in the offshore area of Phu Quy island (Binh Thuan province). The area, alone, can provide the 38.2 GW power generation capacity corresponding to the increasing renewable-energy demand by 2030 planned by the country. There is also a drawback of the wind resource, which is associated with strong multiple-scale temporal variabilities. The seasonal variability associated with monsoon onsets and daily variability associated with the wind diurnal cycles were found ranging 30−50%. Meanwhile, the inter-annual variability could reach up to 10%. These variabilities must be considered when designing wind farms and grids over the region. Additionally, due to the fact that the WRF model performed climatological features of the winds well against the observations, this results indicate that it can be useful tools for wind-power assessment as compared to other reanalysis or QuikSCAT data with coarser spatio-temporal resolutions.

(**Citation**: Doan, V. Q., V. N. Dinh, H. Kusaka, T. Cong, A. Khan, D. V. Toan, and N. D. Duc, 2019: Usability and challenges of offshore wind energy in Vietnam revealed by the regional climate model simulation. *SOLA*, **15**, 113−118, doi:10.2151/sola.2019-021.)

1. Introduction

Vietnam has been experienced fast economic development during the last several decades with the energy consumption increasing constantly year by year. Most of energy consumptions now are provided by hydro- and fossil-fuel powers (GIZ 2016). However, due to their negative impacts on environment and ecology, renewable energy resources, in particular wind energy, are becoming important to maintain a sustainable development of the country (Dinh and McKeogh 2018; Dinh and Nguyen 2018).

A drawback of wind energy is its high dependence on wind that fluctuates greatly at all time scales: seconds, minutes, hours, days, months, seasons and years (Ohba et al. 2016; Doan et al. 2019). Understanding wind temporal variations is of key importance for the integration and optimal utilization of wind in the power system (Foley et al. 2012). Recently, offshore wind has gained increasing attention because of its relatively higher stability compared to onshore wind (Dvorak et al. 2010; Jacobson and Delucchi 2011), and the technological improvement enables cutting the building cost of an offshore wind farm.

The biggest issue of offshore wind resource assessment is a lack of observational wind data, especially those at turbine heights (Mattar and Borvaran 2016). The observed wind data, in most cases, are very limited in terms of time and space and they are difficult to be used for assessing the wind potential for a broad region. Moreover, a precise assessment requires wind data enabling to encompass a long enough time period with high enough temporal frequency in order to capture the multiple-scale temporal variabilities (Argüeso et al. 2018).

Assessment of offshore wind power in Vietnam may be difficult because, firstly, the country has more than 3000 km of coastline, following the Truong Son mountain range stretching from north to south. In many places, the complex coast's terrain can affect the distribution of offshore winds. Secondly, the country is located in the tropical monsoon region with two distinct wind directions, southwest in the summer months and northeast in the winter months. The annual cycle of seasons implies a strong variability in winds putting a challenge on the stable and efficient operation of wind power plants.

Recently, numerical modelling approach with regional climate models (RCMs) has been adopted to assess the offshore wind recourses. RCMs are powerful to generate complete and physically consistent wind data. RCMs allow to estimate winds at given turbine-hub heights, they can also reproduce long-term time series of high frequency outputs, both in time and space. Some successful examples of the modeling approach for assessing wind power potential are Carvalho et al. (2014) for Portugal, Nawri et al. (2014) for Ireland, Yamaguchi et al. (2014) for Japan, Mattar et al. (2016) for Chile, Fant et al. (2016) for South Africa, Giannaros et al. (2017) for Greece, and Argüeso et al. (2018) for Hawaii, USA.

However, none of such above studies having focused on the offshore wind energy in the Southeast Asia. One exception is the recent study of Doan et al. (2018) that has attempted to simulate the offshore wind over the area limited to the Southern Vietnam using a RCM. However, in their study, the simulated wind data have not been validated against observations. It is still unknown how the numerical modelling approach can perform the wind climate in this region. Besides, even though the numerical simulations in the previous studies are valuable assessing the offshore wind potential, none other than that of Argueso et al. (2018) was run over periods that exceeded a year, thus, they do not provide data on the long-term variability and may lack statistical robustness for wind energy analysis. These study gaps need to be filled. On the other hand, from a practical point of view, the assessment of offshore wind resources in Vietnam is also an urgent issue to cope with the rapidly increasing renewable-energy demand associated with economic development.

This study assesses the offshore-wind-power potential over

Corresponding author and present affiliation: Van Q. Doan, Centre for Climate Research Singapore, 36 Kim Chuan Rd, Singapore 537054. E-mail: doan_quang_van@nea.gov.sg.

©The Author(s) 2019. This is an open access article published by the Meteorological Society of Japan under a Creative Commons Attribution 4.0 International (CC BY 4.0) license (http://creativecommons.org/license/by/4.0).

the sea of Vietnam using a state-of-art regional climate model, the Weather Research and Forecasting (WRF) model. The numerical simulation is run for 10-year period (2006−2015) with the finest resolution of 10 × 10 km that cover whole the Vietnam region to have robust wind data for analyzing. The variabilities of wind power potential in space and time at multiple scale from inter-annual to hourly are fully characterized. To the best of our knowledge, this is the first study describing the offshore wind power generation capacity in the Vietnam region from the climatological view using a numerical method. The results obtained will be useful for the policy makers as well as developers seeking optimal placement of offshore wind farms.

2. Methods

2.1 Atmospheric model and simulation design

The Weather Research and Forecast (WRF) model version 3.5.1 was used to reproduce the wind climate over the Vietnam region. Model configurations are shown in Table 1. The model includes two nested grids with grid spacing of the inner most domain 10 × 10 km (Fig. 1). Slide runs (for each month) was conducted for ten years 2006 Jan–2015 Dec with the initial and boundary conditions created from the Final (FNL) Operational Global Analysis data of the National Center for Environmental Prediction (NCEP) as the initial and boundary conditions. The NCEP FNL data, which are provided every 6 hours, have horizontal resolution of 1 × 1 degree (NCEP 2000). The 10-year simulation period is expected to provide robust enough results to characterize the spatial and seasonal variability of wind field over the region.

The physical schemes is chosen for popularity in wind simulation that was confirmed in many previous studies (Argüeso et al. 2018). The Yonsei University (YSU) Planetary Boundary Layer (PBL) scheme (Hong et al. 2006) was used to represent the turbulence in the atmosphere boundary layer. The WRF Single-Moment 6-Class Microphysics (WSM-6) scheme (Hong and Lim 2006) was chosen to solve cloud microphysics processes. The Rapid Radiative Transfer Model (RRTM) for longwave radiation and the Dudhia scheme for shortwave radiation were used for their efficiency and good performance for wind simulations (Guo and Xiao 2014; Santos-Alamillos et al. 2013). Convective processes were represented with the Kain-Fritsch cumulus scheme (Kain 2004) for two simulation domains. The Noah Land Surface Model (Chen and Dudhia 2001) was used to simulate the land-atmosphere interactions.

2.2 Observation data

The simulated wind speed was compared to the observational data to evaluate the performance of the WRF model. Two observational data sources were used in this study. The first is the wind data observed at six ground-based weather stations run by the Vietnam Center of Hydro-Meteorological Data (VCHMD). Such stations are located in islands off the coast of Vietnam (see Fig. 1b). The station data are measured four times (00, 06, 12, 18 UTC) a day and available for 10 years 2006−2015.

Another source is the QuikSCAT (Quick Scatterometer) data. QuikSCAT is the NASA's Earth observation satellite carrying the sea winds scatterometer (Draper et al. 2004; Said et al. 2011). QuikSCAT provided the gridded wind speed with two components referenced to 10 meters above the sea surface with global coverage at a spatial resolution of 25 km. Only the data for five years 2006−2010 were used to compared to the simulated data.

2.3 Estimation of wind power potential

Wind power density (WPD), a measure of energy flux through an area perpendicular to the direction of motion, varies with the cube of wind speed and air density. WPD is the defined as,

$$P_{den} = \frac{1}{2}\rho\frac{1}{N}\sum_{i=1}^{N} v_i^3, \qquad (1)$$

Table 1. Model configuration.

	Domain 01	Domain 02
Model	WRF V3.5.1	
Initial/boundary condition	NCEP Final (FNL) reanalysis data	
Simulation period	2006 Jan 01–2015 Dec 31	
Grid spacing	30 km	10 km
Number of grids	150 × 150	220 × 214
Number of vertical layers	38 layers	
Microphysics scheme	WRF single–moment 6–class scheme	
Land surface scheme	Noah land-surface model	
Boundary layer scheme	Yonsei university scheme	
Shortwave radiation	Dudhia scheme	
Longwave radiation	RRTMG Longwave scheme	
Cumulus	Kain–Fritsch scheme	

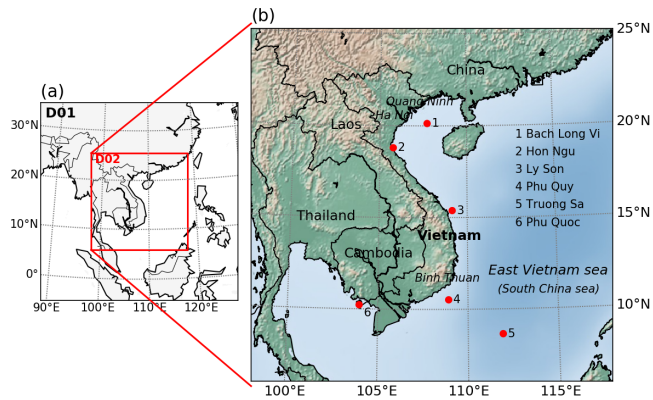

Fig. 1. (a) Configuration of the WRF domains. D01 and D02 stands for domain 01 and 02, having horizontal resolutions of 30 and 10 km, respectively. (b) Detailed map for D02. Red circle markers indicate the location of ground based weather stations in offshore islands of Vietnam. Wind data from such stations are used for validation of the WRF model.

where ρ is the air density assumed constant of 1.225 (kg/m^3); v_i is instantaneous wind speed; N is a total number of hours of the output wind speed data. Wind power density depends on atmospheric variable and is therefore most appropriate for turbine-independent evaluations of wind energy potential.

The turbine chosen for the hypothetical wind farm is Vestas V164-8.0. It has rated power (P_r) of 8 MW with 80 m blade with swept area of 21, 124 m^2. The approximate hub height is 105 m. The turbine is used in use in several offshore wind farms such as Burbo Bank Offshore, the United Kingdom and Norther N.V., Belgium (Aarhus 2019). The turbine starts generating power ($P_f(v)$) at the cut-in wind speed (v_{ci}), of 4 m/s and shuts off at the cut-out wind speed (v_{co}) of 25 m/s. The rated wind speed (v_r) of the turbine is 13 m/s. Using the hourly wind speed data and the power curve of the turbine (Fig. S1 in Supplement), the hourly power production P_i from the turbine is calculated by using Eq. (2).

$$P_i(v,t) = \begin{cases} 0, & v < v_{ci} \\ P_f(v), & v_{ci} \le v < v_r \\ P_r, & v_r \le v < v_{co} \\ 0, & v_{co} \le v \end{cases} \qquad (2)$$

The actual energy output (E) of the wind turbine for N hours can be calculated as

$$E = \sum_{i=1}^{N} P_i \qquad (3)$$

where P_i is the hourly power production. N is number of hours.

3. Results and discussions

3.1 Model validation

Figure 2 shows the probability distribution of the modeled and station observed wind speed. The model, overall, appears to perform well the observed wind speed climate. Especially, there is good matching in the shapes of probability distribution between the modelled and the observed data, in particular, at Phu Quy, Truong Sa, Phu Quoc. However, it is likely that there also exists positive biases (defined as the modelled result minus the observation) over most stations, systematically. Biases range from 0.9 m/s at Phu Quoc to 3.5 m/s at Phu Quy (Table 2). To explain these biases, it is worthwhile to remind that all 6 weather stations are located in small islands of the Vietnam sea (Fig. 1b). However, having the resolution of 10 × 10 km, the WRF model is unable to resolve these islands. The land use categories of grid points, corresponding to the location of weather stations, were classified as water surface rather than land (Table 2) in the model.

Additional sensitivity simulations with nesting to finer resolutions demonstrated that the misrepresentation of island land use as water surface could induce underestimation of the surface friction thus resulting in the overprediction of surface wind speed (Fig. S2 in Supplements). This result is consistent with the finding by Santos-Alamillos (2015). On the other hand, the wind speed at upper air levels has been predicted more consistently by WRF at different resolutions (Fig. S2).

Figure 3 shows the comparison between the modelled data and the QuikSCAT data. Much better agreement between two wind speed datasets are seen, the biases are much smaller than

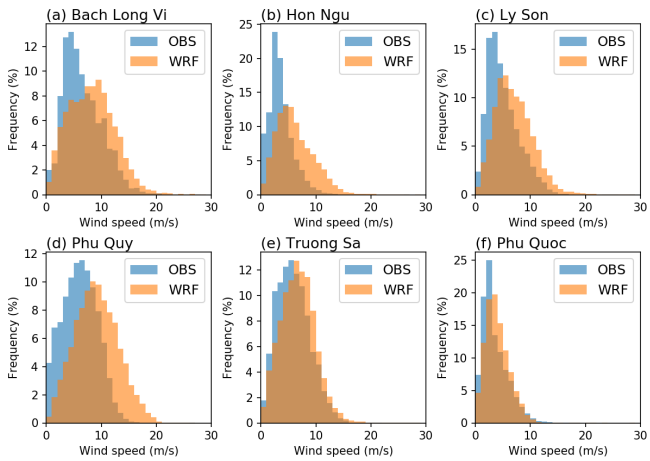

Fig. 2. Probability distribution of the simulated (WRF) and observed (OBS) surface wind speed data at six stations. Data are four times per day (00, 06, 12, and 18 UTC) for 10 years 2006−2015.

Table 2. List of ground-based weather stations.

Station	Latitude	Longitude	Model land use	Wind speed bias (m/s)
Bach Long Vi	20.13	107.72	Water surface	2.2
Hon Ngu	18.8	105.77	Water surface	3.1
Ly Son	15.38	109.15	Water surface	2.5
Phu Quy	10.52	108.93	Water surface	3.5
Truong Sa	8.65	111.92	Water surface	1.3
Phu Quoc	10.22	103.97	Forest (ever-green broadleaf)	0.9

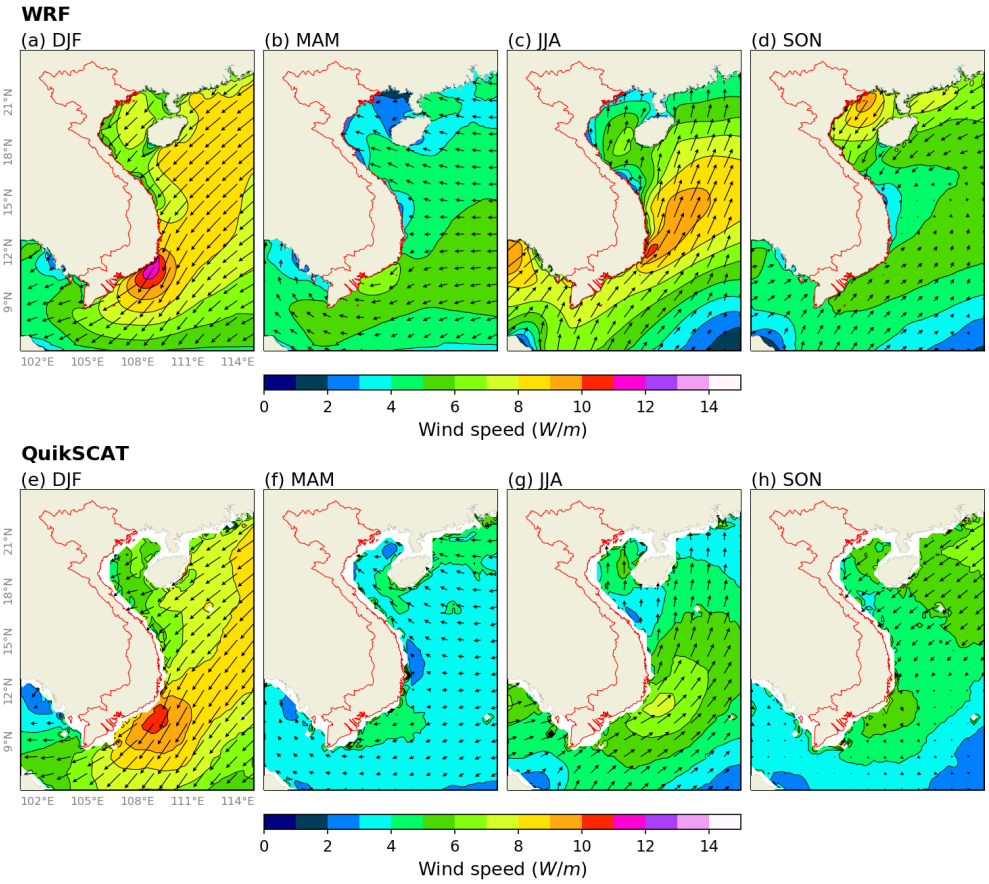

Fig. 3. Spatial distribution of seasonal mean surface wind speed from the WRF and the QuikSCAT data. Data was averaged for five years 2006−2010.

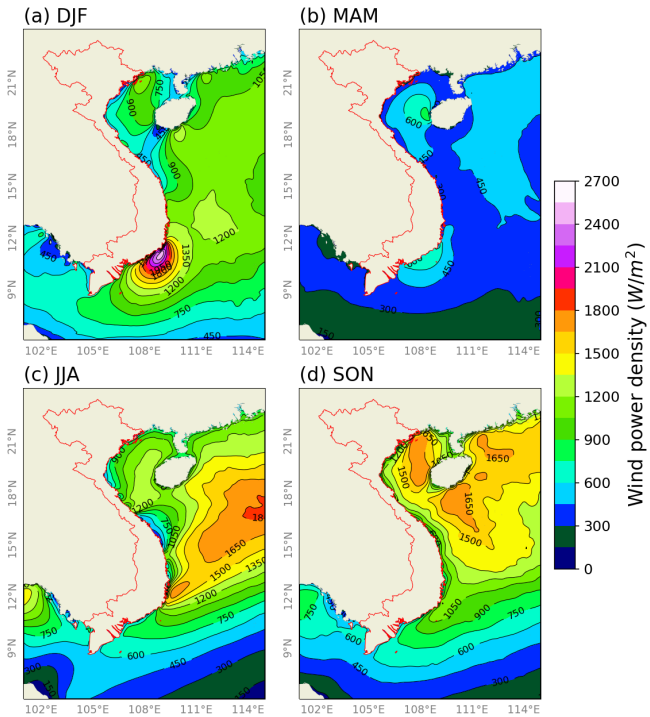

Fig. 4. Spatial distribution of seasonal mean wind power density calculated at the hub height.

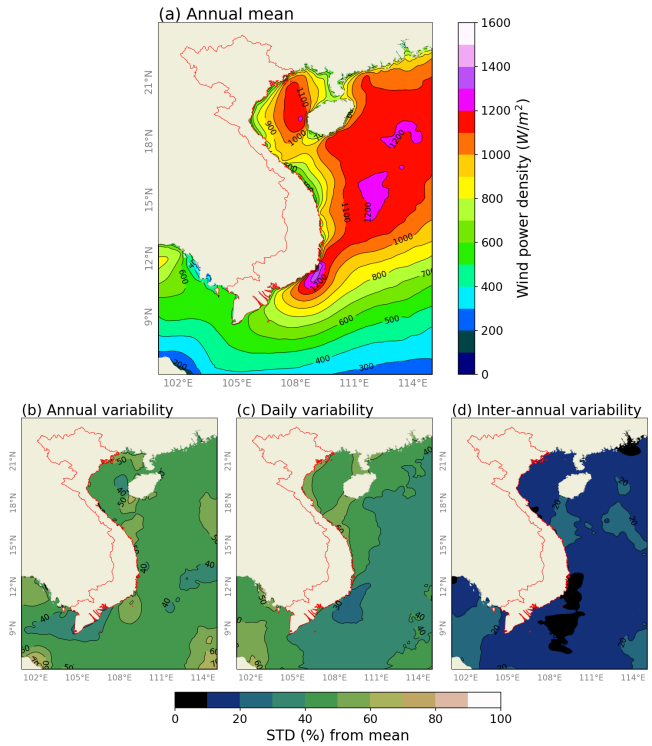

Fig. 5. (a) Spatial distribution of the annual mean wind power density at the turbine hub height; (b) seasonal variability, defined as the normalized standard deviation of the monthly mean values; (c) daily variability, defined as the normalized standard deviation of hourly data; (d) inter-annual variability, defined as the normalized standard deviation of yearly mean from 10-year mean.

that when compared with station data. The mean bias of the WRF model versus the QuikSCAT data was only 0.84 m/s (Fig. S3 in Supplements). The WRF model shows a good performance in terms of either wind speed or direction. The seasonal variation, which is due to the dominant northeastern monsoon during the winter months December–January–February (DJF), and southwestern monsoon during summer months June–July–August (JJA) was well predicted by the model. The lower wind speed in the inter-monsoon months, March–April–May (MAM) and September–October–November (SON) are seen in both the WRF and the QuikSCAT data. However, there is small overestimation of wind speed during MAM.

The largest wind speed is seen in the offshore area of Phu Quy island (Binh Thuan province in the south), followed by that of Bach Long Vi island (Quang Ninh province in the north) (Fig. 4). The maximum surface wind speed at Phu Quy could reach 10 m/s in DFJ; whereas, the maximum at Bach Long Vi was 9 m/s in SON.

3.2 Wind power density

The WPD calculated from the simulated wind speed at the hub height (105 m) is shown in Fig. 4. Overall, the offshore wind power potential in Vietnam is characterized by the strong heterogeneity both in space and time. The consistently high value is seen in the area of the Phu Quy island where the WPD could reach above 2000 W/m^2 during DFJ (Fig. 4a) with the annual mean of 1200 W/m^2 (Fig. 5a). In the north, the higher value is seen over the Bach Long Vi island, where it could reach above 1200 W/m^2 during SON and the annual mean was greater than 1000 W/m^2. The offshore areas of the northern and central parts had the relatively lower WPD with the annual mean ranging 600−700 W/m^2 (Fig. 5a). During inter-monsoon months, i.e., MAM and SON, the WPD was lower and more spatially homogeneous (Figs. 4b and 4d).

Temporal variabilities of wind power generation is important in designing efficient wind power plants. Here, the annual variability (Fig. 5b), i.e., the variation within the annual cycle, of the WPD is defined as the normalized standard deviation of monthly means, the daily variability (Fig. 5c) defined as the normalized standard deviation of hourly data from the daily mean; the inter-annual variability (Fig. 5d) defined as the normalized standard deviation of yearly means during 10-year period 2006−2015.

The variabilities at multiple temporal scales look more spatially identical. The annual variability ranged 40−50%, and the daily variability ranged 30−50% (Figs. 5b and 5c). The Southeast monsoon circulation, with dominant northeasterly wind during DJF and southwesterly wind during JJA, is a reason for the annual variability of WPD over the offshore area of Vietnam.

The comparison between the simulation versus the station observations and the QuikSCAT data demonstrated the good performance on the annual and daily variabilities (Figs. S4 and S5), though the model tended to overestimate the absolute WPD values. The overestimation is seen in particular over Hon Ngu and Ly Son islands, which are located relatively close to the land. Meanwhile, the model tended to underestimate WPD over Truong Sa island which is located far away into the East Vietnam.

The inter-annual variability of WPD ranged 10−30% lower than the annual and daily variabilities. The inter-annual variability of WPD is strongly influenced by cross-equatorial flow in the Indian ocean and negatively correlated with trade wind over the western Pacific ocean during JJA. In contrast, it is highly affected by the Asia continent high pressure during DJF (Fig. S6).

3.3 Wind power generation

Turbine Vestas V164-8.0, which has the hub height of 105 m and the rated power of 8 MW, was chosen for the hypothetical wind farm. The turbine is able to generate power at the "effective" wind speed, i.e., between the cut-in 4 m/s and the cut-out 25 m/s. Understanding the frequency, or fraction of "effective" wind speed to total time, is important for efficient use of the wind turbine.

The simulated results show the strong variation of "effective" wind speed frequency over space and time (Fig. S7). The highest frequency is seen over the offshore area of Binh Thuan province, which could reach above 95% in monsoon months, i.e., DFJ and

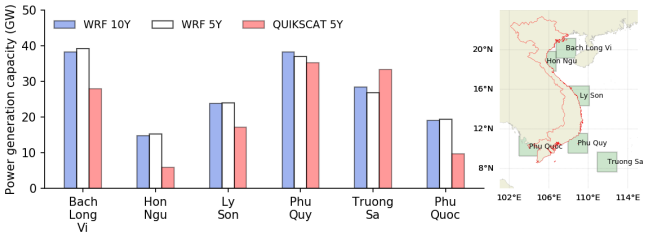

Fig. 6. Power generation capacity in areas of 6 islands. The power capacity is integrated by entire offshore area (within the box of 200 × 200 km) assumed hypothetical turbine Vestas V164-8.0 and the maximum 2 turbines is installed into 1 km^2. WRF 10 Y represents the 10-year (2006−2015) mean WRF data; WRF 5 Y and QUIKSCAT 5 Y are the 5-year (2006−2010) mean of WRF and QuikSCAT data, respectively.

JJA, and being lower about 60−80% in inter-monsoon months, i.e., MAM and SON. Interestingly, the frequency was very high of 95 % over Phu Quoc island (southwestern coast) in JJA. This was comparable with that over the offshore area of Binh Thuan province, in spite of the lower the mean WPD observed here (Fig. 4c).

The wind power generation ability was analyzed. Assume the hypothetical turbines are installed over the area of six islands (Fig. 6). The simulated result shows that the sea areas of Bach Long Vi and Phu Quy islands can provide the power generation capacity of 38.2 GW, which itself can contribute significantly to the national installed power capacities of 60 GW in 2020 and 130 GW in 2030 as in the latest PDP in Vietnam (GIZ 2016). Note that simulated wind power generation is likely higher than that calculated for the QuikSCAT data (using power-law wind profile with an exponent of 0.11 for wind over open water according to Hsu et al. 1993).

4. Conclusions

This study assessed the offshore-wind-power potential in the Vietnam sea by using the numerical modelling approach with the WRF model. The findings revealed in this study are described as following.

- Vietnam has high potential of offshore wind energy with the wind power density greater than 400 W/m^2 in most offshore areas. However, the wind power potential has strong spatial heterogeneity because of long and narrow geographical characteristics of the country with more than 3000 km long south-north coastline. The largest annual mean wind power density of above 1000 W/m^2 was found near to Phu Quy island (Binh Thuan province) and Bach Long Vi island (Quang Ninh province). The area surrounding Phu Quy island, alone, can provide the power generation capacity of 38.2 GW with the hypothetical wind turbine Vestas V164-8.0.
- This study highlighted the drawback of offshore wind power associated with the large temporal variabilities. The annual and daily variabilities are high about of 30−50%. The inter-annual variability is about 10−30%. These variabilities should be carefully considered when designing wind farms and grids over the region.
- The results obtained in this study can be a useful guideline for policy makers in building the strategy of renewable energy infrastructure in Vietnam as well as for developers who needs high-quality offshore wind power atlas to identify suitable locations of wind farms. In addition, this highlighted the great potential using numerical models for assessing the wind and wind power resources in Vietnam as well as the other Southeast Asia countries in the tropical-monsoon climate zone where lack of the offshore in-situ measurement network.

Acknowledgement

This work was supported by the "Interdisciplinary Computational Science Program" in the Center for Computational Sciences, University of Tsukuba. The second author (V.N. Dinh) has been funded by Science Foundation Ireland (SFI) Research Centre: MaREI - Centre for Marine and Renewable Energy (12/RC/2302).

Edited by: A. Manda

Reference

Aarhus, 2019: World's most powerful wind turbine selected for Belgium's largest offshore wind park (Available online at http://www.mhivestasoffshore.com/norther-foi/, accessed 12 April 2019).

Argüeso, D., and S. Businger, 2018: Wind power characteristics of Oahu, Hawaii. *Renewable Energy*, **128**, 324−336.

Balog, I., P. M. Ruti, I. Tobin, V. Armenio, and R. Vautard, 2016: A numerical approach for planning offshore wind farms from regional to local scales over the Mediterranean. *Renewable Energy*, **85**, 395−405.

Carvalho, D., A. Rocha, M. Gómez-Gesteira, and C. S. Santos, 2014: WRF wind simulation and wind energy production estimates forced by different reanalyses: Comparison with observed data for Portugal. *Applied Energy*, **117**, 116−126.

Chen, F., and J. Dudhia, 2001: Coupling an advanced land surface-hydrology model with the Penn State-NCAR MM5 modeling system. Part II: Preliminary model validation. *Mon. Wea. Rev.*, **129**, 587−604.

Dinh, V. N., and E. McKeogh, 2018: Offshore wind energy: Technology opportunities and challenges. *Lecture Notes in Civil Engineering, Proc. the Vietnam Symposium on Advances in Offshore Engineering*, **18**, 3−22, doi:10.1007/978-981-13-2306-5_31.

Dinh, V. N., and H. X. Nguyen, 2018: Design of an offshore wind farm layout. *Lecture Notes in Civil Engineering, Proc. the Vietnam Symposium on Advances in Offshore Engineering*, **18**, 233−238, doi:10.1007/978-981-13-2306-5_31.

Doan, V. Q., H. Kusaka, T. V. Du, D. D. Nguyen, and T. Cong, 2018: Numerical approach for studying offshore wind power potential along the southern coast of Vietnam. *Lecture Notes in Civil Engineering, Proc. the Vietnam Symposium on Advances in Offshore Engineering*, **18**, 245−249.

Doan, V. Q., H. Kusaka, M. Matsueda, and R. Ikeda, 2019: Application of mesoscale ensemble forecast method for prediction of wind speed ramps. *Wind Energy*, doi:10.1002/we.2302.

Draper, D. W., and D. G. Long, 2004: Evaluating the effect of rain on SeaWinds scatterometer measurements. *J. Geophys. Res.*, **109**, 1−12, doi:10.1029/2002JC001741.

Dvorak, M. J., C. L. Archer, and M. Z. Jacobson, 2010: California offshore wind energy potential. *Renewable Energy*, **35**, 1244−1254.

Fant, C., C. A. Schlosser, and K. Strzepek, 2016: The impact of climate change on wind and solar resources in southern Africa. *Appl. Energy*, **161**, 556−564.

Foley, A. M., P. G. Leahy, A. Marvuglia, and E. J. McKeogh, 2012: Current methods and advances in forecasting of wind power generation. *Renewable Energy*, **37**, 1−8.

Giannaros, T. M., D. Melas, and I. C. Ziomas, 2017: Performance evaluation of the Weather Research and Forecasting (WRF) model for assessing wind resource in Greece. *Renewable Energy*, **102**, 190−198.

Gesellschaft für Internationale Zusammenarbeit (GIZ), 2016: Vietnam Power Development Plan for the Period 2011−2010: Highlights of the PDP 7 revised. GIZ Energy Support Programme in Viet Nam (Available online at http://gizenergy.org.vn, accessed 12 April 2019).

Guo, Z., and X. Xiao, 2014: Wind power assessment based on a WRF wind simulation with developed power curve modeling methods. *Abstract and Applied Analysis*, **2014**, 1−15.

Hennessey, J., 1977: Some aspects of wind power statistics. *J. Appl. Meteor.*, **16**, 119−128.

Hong, S., and J. Lim, 2006: The WRF single-moment 6-class microphysics scheme (WSM6). *J. Korean Meteor. Soc.*, **42**, 129−151.

Hong, S.-Y., Y. Noh, and J. Dudhia, 2006: A new vertical diffusion package with an explicit treatment of entrainment processes. *Mon. Wea. Rev.*, **134**, 2318−2341.

Hsu, S. A., E. A. Meindl, and D. B. Gilhousen, 1994: Determining the power-law wind-profile exponent under near-neutral stability conditions at sea. *J. Appl. Meteor. Climatol.*, **33**, 757−765.

Jacobson, M. Z., and M. A. Delucchi, 2011: Providing all global energy with wind, water, and solar power, Part I: Technologies, energy resources, quantities and areas of infrastructure, and materials. *Energy Policy*, **39**, 1154−1169.

Kain, J. S., 2004: The Kain-Fritsch convective parameterization: an update. *J. Appl. Meteor.*, **43**, 170−181.

Koplitz, S. N., D. J. Jacob, M. P. Sulprizio, L. Myllyvirta, and C. Reid, 2017: Burden of disease from rising coal-fired power plant emissions in Southeast Asia. *Environ. Sci. Technol.*, **51**, 1467−1476, doi:10.1021/acs.est.6b03731.

Mattar, C., and D. Borvarán, D., 2016: Offshore wind power simulation by using WRF in the central coast of Chile. *Renewable Energy*, **94**, 22−31.

National Centers for Environmental Prediction, 2000: *NCEP FNL Operational Model Global Tropospheric Analyses, continuing from July 1999* (Available online at https://doi.org/10.5065/D6M043C6, accessed 12 April 2019).

Nawri, N., G. N. Petersen, H. Björnsson, A. N. Hahmann, K. Jónasson, C. B. Hasager, and N. E. Clausen, 2014: The wind energy potential of Iceland. *Renewable Energy*, **69**, 290−299.

Ohba, M., S. Kadokura, and D. Nohara, 2016: Impacts of synoptic circulation patterns on wind power ramp eventsin East Japan. *Renewable Energy*, **96**, 591−602.

Said, F., and D. G. Long, 2011: Determining selected tropical cyclone characteristics using QuikSCAT's ultra-high resolution images. *IEEE Journal of Selected Topics in Applied Earth Observations and Remote Sensing*, **4**, 857−869.

Santos-Alamillos, F. J., D. Pozo-Vázquez, J. A. Ruiz-Arias, V. Lara-Fanego, and J. Tovar-Pescador, 2013: Analysis of WRF model wind estimate sensitivity to physics parameterization choice and terrain representation in Andalusia (Southern Spain). *J. Appl. Meteor. Climatol.*, **52**, 1592−1609.

Santos-Alamillos, F., D. Pozo-Vázquez, J. Ruiz-Arias, and J. Tovar-Pescador, 2015: Influence of land-use misrepresentation on the accuracy of WRF wind estimates: Evaluation of GLCC and CORINE land-use maps in southern Spain. *Atmos. Res.*, **157**, 17−28.

Wind turbines database, 2019: Ventas V164-8.0 (Available online at https://en.wind-turbine-models.com/turbines/318-vestas-v164-8.0, accessed 12 April 2019).

Yamaguchi, A., and T. Ishihara, 2014: Assessment of offshore wind energy potential using mesoscale model and geographic information system. *Renewable Energy*, **69**, 506−515.

Manuscript received 28 February 2019, accepted 13 April 2019
SOLA: *https://www.jstage.jst.go.jp/browse/sola/*